

## Frequency-Dependent Thermal Response of the Charge System and the Restricted Sum Rules of $\text{La}_{2-x}\text{Sr}_x\text{CuO}_4$

M. Ortolani, P. Calvani, and S. Lupi

"Coherentia"—INFM and Dipartimento di Fisica, Università di Roma La Sapienza, Piazzale Aldo Moro 2, I-00185 Roma, Italy  
(Received 16 July 2004; published 14 February 2005)

In  $\text{La}_{2-x}\text{Sr}_x\text{CuO}_4$  (LSCO) the spectral weight  $W = \int_0^\Omega \sigma_1^{ab}(\omega, T) d\omega$  [where  $\sigma_1^{ab}(\omega, T)$  is the  $ab$ -plane conductivity] obeys the same law  $W = W_0 - B(\Omega)T^2$  as in a conventional metal such as gold, for any  $\Omega$  up to the plasma edge. However, in LSCO  $B(\Omega)$  points toward correlation effects and, unlike in gold, is related to an energy scale  $t_T \ll t_0 \sim W_0$ . The Ferrell-Glover-Tinkham sum rule is fulfilled in LSCO superconductors for  $\Omega \gtrsim 2000 \text{ cm}^{-1}$ .

DOI: 10.1103/PhysRevLett.94.067002

PACS numbers: 74.25.Gz, 74.25.Kc, 74.72.-h

The optical properties of high- $T_c$  cuprates, both in the normal and in the superconducting phase, are still extensively discussed in the literature. For  $T > T_c$ , an infrared conductivity  $\sigma_1^{ab}(\omega)$  peaked at  $\omega = 0$  and smoothly decreasing with  $\omega$  supports one-component approaches [1]. In other experiments, contributions peaked at finite frequencies show up [2,3], which point towards charge localization and ordering. Below  $T_c$ , contradictory results are reported on the London penetration depth [4,5] extracted from  $\sigma_1^{ab}(\omega)$ .

Therefore, recent works have been often focused on a model-independent quantity such as the spectral weight

$$W(\Omega, T) = \int_0^\Omega \sigma_1(\omega, T) d\omega \quad (1)$$

and on its behavior in different spectral ranges. For  $\Omega \rightarrow \infty$ , the sum rule on the real part of the optical conductivity  $\sigma_1(\omega, T)$  requires that  $W(\Omega, T)$  is independent of temperature. However, there are a few special cases where "restricted sum rules" can be considered. In metals  $W(\omega_p)$ , where  $\omega_p$  is the plasma frequency which approximately coincides with the minimum in the reflectivity (plasma edge), is expected to be nearly independent of  $T$  [6]. Another example is the Ferrell-Glover-Tinkham (FGT) sum rule which predicts that the  $W$  lost at low energy when a superconductor is cooled below  $T_c$  is recovered in the  $\delta$  function at  $\omega = 0$ .

In cuprates such as  $\text{Bi}_2\text{Sr}_2\text{CaCu}_2\text{O}_{8+y}$  (BSCCO) and  $\text{YBa}_2\text{Cu}_3\text{O}_{7-y}$  the restricted sum rules have been investigated by several groups [7–10]. In  $\text{La}_{2-x}\text{Sr}_x\text{CuO}_4$  (LSCO), a similar study on the in-plane  $\sigma_1^{ab}(\omega)$  has recently appeared [5], while a previous work was focused on the  $c$ -axis conductivity [11]. In the present Letter we study the behavior of  $W(\Omega, T)$  in LSCO. In the normal phase, starting from the sum rule restricted to  $\omega_p$ , we observe topic differences between LSCO, BSCCO, and conventional metals, which lead us to identify two different energy scales for the charge system in the cuprates. In the superconducting phase we find that the FGT sum rule holds only if the frequency range is extended well above  $2000 \text{ cm}^{-1}$ .

The reflectivity  $R_{ab}(\omega)$  of the two LSCO single crystals (a superconductor with  $x = 0.12$  and a nonsuperconducting metal with  $x = 0.26$ ) were measured with respect to that of a gold film (between 15 and  $12\,000 \text{ cm}^{-1}$ ) and a silver film (up to  $20\,000 \text{ cm}^{-1}$ ), both of which evaporated *in situ* onto the sample. The reflectivity of gold was then measured with respect to a platinum mirror, both in order to correct for its  $\omega$  dependence in the near infrared and to compare the response of LSCO at  $x = 0.26$ , which is often indicated as a "normal metal" with that of a good conventional metal. The optical configuration for measuring  $R_{ab}(\omega)$  in LSCO is shown in the inset of Fig. 1(a). The radiation impinges under an incidence angle of  $8^\circ$  on the surface of the crystal. By use of a four-circle diffractometer and a laser we determined for  $x = 0.12$  a miscut of  $\theta = 1.0^\circ \pm 0.5^\circ$  with respect to an ideal  $ab$  plane. Therefore, we used a polarizer to align the electric field orthogonally to the miscut plane. We show elsewhere [12] that, under these conditions, the relative deviation with respect to the ideal reflectivity of the  $ab$  plane is

$$\frac{\Delta R_{ab}(\omega)}{R_{ab}(\omega)} \simeq \sqrt{2(1-\eta)} \frac{1-R_{ab}^2(\omega)}{R_{ab}(\omega)} \theta^2 g(\omega). \quad (2)$$

Here,  $\eta = (I_p - I_u)/(I_p + I_u)$ , as  $I_p$  ( $I_u$ ) is the intensity of the field component parallel (orthogonal) to the polarizing direction. It is plotted in the inset (gray lines) for both the polyethylene and the KRS-5 device here used. Moreover,

$$g(\omega) = \left[ \frac{-2\omega}{\pi \epsilon_2^{ab}} \wp \int_0^\infty \frac{-(\epsilon_1^{ab})^2/2\epsilon_1^c}{\omega'^2 - \omega^2} d\omega' + \frac{1}{2} \right]. \quad (3)$$

$\Delta R_{ab}(\omega)/R_{ab}(\omega)$  turns out to be [12] on the order of 0.001 at  $100 \text{ cm}^{-1}$ , much smaller than the experimental noise. In fact, no signature of the  $c$ -axis phonons appears in the  $R_{ab}(\omega)$  of the  $x = 0.12$  sample (see the top inset of Fig. 1). In previous measurements on the  $ac$  surface of the same sample, reported in Ref. [3], a dip from such a phonon appeared around  $470 \text{ cm}^{-1}$  [13]. In that case, however, the commercial polyethylene polarizer was used in its whole transmittance range. As shown in the inset,  $\eta$  drops to 0.93 at that frequency, causing a 4% deviation from the real reflectivity of the  $a$  axis. Below

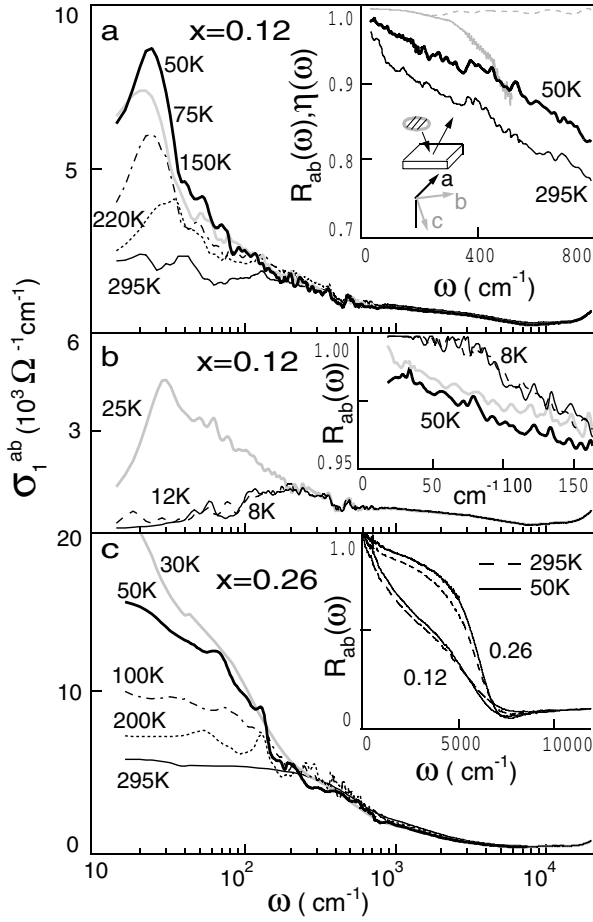


FIG. 1. Optical conductivity, from the reflectivity data reported in the inset, of the underdoped crystal  $x = 0.12$  above  $T_c$  (a) and below  $T_c$  (b) compared with that of the nonsuperconducting metal  $x = 0.26$  (c). The insets show the corresponding  $R_{ab}$ : in the far infrared (FIR) for  $x = 0.12$  (a) above and (b) below  $T_c$ ; in the whole energy range for both  $x = 0.12$  and  $0.26$  (c). In the inset of (a) the gray lines plot the efficiency  $\eta$  of the polarizers employed in the experiment: polyethylene (solid line) and KRS-5 (dotted line).

$200 \text{ cm}^{-1}$ , where  $\eta > 0.99$ , the results of Ref. [3] on this one and other samples were not affected by the  $c$ -axis response. This is confirmed by the results with the present safe procedure, which was applied to both  $x = 0.12$  and  $0.26$ . In the former one the in-plane conductivity  $\sigma_1^{ab}(\omega)$ , once extracted from the  $R_{ab}(\omega)$  extrapolated to  $\omega = 0$  by a Drude-Lorentz fit, shows again [Fig. 1(a)] the  $T$ -dependent resonance at  $\approx 30 \text{ cm}^{-1}$  reported in Ref. [3] for this and other LSCO samples. The resonance is not observed in the nonsuperconducting metal with  $x = 0.26$  [Fig. 1(c)]. A discussion of the FIR peak and of other details of the LSCO conductivity is reported in Refs. [3,14]. They are not relevant to the present study of the spectral weight in LSCO, a quantity insensitive to narrow spectral features in the far infrared.

In both samples of Fig. 1, the screened plasma frequency  $\tilde{\omega}_p$  obtained from the condition  $\epsilon_1(\omega) \approx 0$  (for a scattering

rate  $\Gamma \ll \tilde{\omega}_p$ ) is  $6100 \pm 150 \text{ cm}^{-1}$ , independent of  $T$  within errors. This is in agreement with the value ( $6300 \pm 100 \text{ cm}^{-1}$ ) extracted from a Drude fit in LSCO films with different doping [4]. However, in order to include the whole free-carrier contribution in Eq. (1), we followed Ref. [15] and extended the integration limit  $\Omega$  to the  $\omega_p$  corresponding to the minimum in the reflectivity (plasma edge). In the inset of Fig. 1(c), this gives  $6800 \text{ cm}^{-1}$  for both samples. In conventional metals  $W$  exhibits a temperature dependence

$$W(\Omega = \omega_p, T) \approx W_0 - BT^2, \quad (4)$$

where  $W_0$  accounts for all the carriers in the conduction band, while  $B$  depends crucially on the density of states at the Fermi energy  $\rho(E_F)$ . In a tight-binding approach *both*  $W_0$  and  $B$  depend on the same hopping rate  $t_0$ . Equation (4) is verified in gold, as one can see from our data in Fig. 2(c) where  $\omega_p = 20\,500 \text{ cm}^{-1}$  (from the zero crossing of  $\epsilon_1$ ).

It has been found that Eq. (4) holds also for a high- $T_c$  superconductor such as BSCCO [8,15]. Here, Figs. 2(d) and 2(e) show that this behavior is verified also in LSCO, both for  $x = 0.26$  and  $x = 0.12$ . One may ask if these findings are sufficient to extend the above tight-binding approach, characterized by a single energy scale  $t_0$ , to cuprates. To obtain deeper insight, we notice that for LSCO, based on the good fits in Figs. 2(d) and 2(e), the above  $T^2$  dependence holds [16] not only at  $\omega_p$ , but also

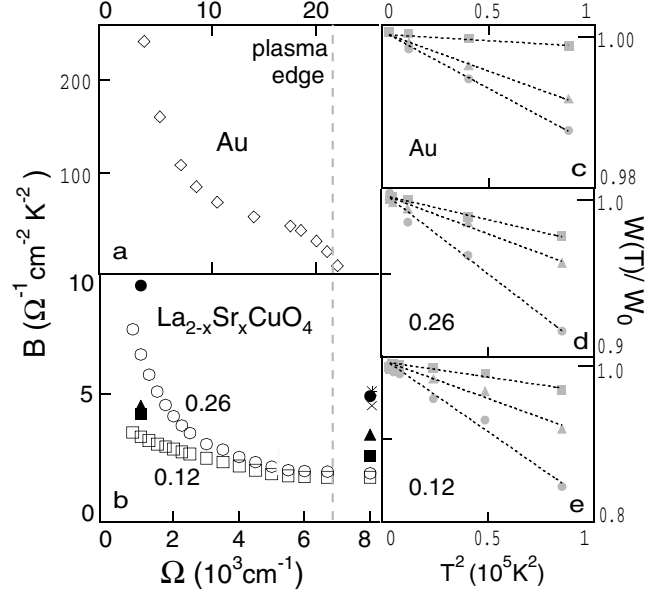


FIG. 2. The coefficient  $B(\Omega)$  in Eq. (4) is plotted for gold (a), and LSCO with  $x = 0.12$  and  $0.26$  (b), as extracted from plots like those in (c), (d), and (e), respectively. Therein, gray squares refer to  $\Omega = \omega_p$ , triangles to  $\Omega = 0.5\omega_p$ , and circles to  $\Omega = 0.2\omega_p$ . In (b),  $B$  values obtained from the existing data on  $\text{Bi}_2\text{Sr}_3\text{CaCu}_2\text{O}_{8+y}$  with different  $y$  and  $T_c$  are reported for comparison: full symbols are from Ref. [7] (circles,  $T_c = 70 \text{ K}$ ; triangles,  $80 \text{ K}$ ; squares,  $63 \text{ K}$ ); the star ( $T_c = 88 \text{ K}$ ) and the cross ( $66 \text{ K}$ ) are extracted from the data of Ref. [8].

for lower values of  $\Omega$  (provided that they are higher than the highest phonon frequency,  $\sim 700 \text{ cm}^{-1}$ ). Therefore, we can write for both gold and LSCO

$$W(\Omega, T) \simeq W_0 - B(\Omega)T^2. \quad (5)$$

The frequency-dependent coefficient  $B(\Omega)$ , which we introduce through Eq. (5), describes the “thermal response” of the carriers. It can be evaluated at any  $\Omega$  as done in Figs. 2(c)–2(e). The resulting values are reported in the left panels of the same figure. In gold (a), all  $T$ -dependent mechanisms are confined at  $\omega \lesssim \omega_p$  and at the plasma edge,  $B \simeq 0$ . In both LSCO samples, on the contrary, at the edge  $B$  is still much different from zero [ $B(\omega_p) = 1.7 \text{ } \Omega^{-1} \text{ cm}^{-2} \text{ K}^{-2}$ ]. (When evaluating these figures one should consider that the  $B$  scale for gold is larger by more than a factor of 10 than in LSCO, as  $W_0 \propto \omega_p^2$ .) The result at  $\omega_p$  is not surprising, in view of the correlation effects that, in LSCO, may extend the  $T$  dependence of the carrier response up to energies on the order of the Hubbard splitting  $U$ . One should then observe similar effects in other cuprates. Indeed, by using the data of Refs. [8,15] on five BSCCO samples with different  $T_c$ 's, one obtains the  $B$  values shown for comparison in Fig. 2(b). All of them, at the BSCCO  $\omega_p \sim 8000 \text{ cm}^{-1}$ , are even higher than here found in LSCO.

One may ask if the predictions of the noninteracting, tight-binding model for the Cu-O square lattice are compatible with these results. For the present purpose one can use a simplified one-band picture and obtain

$$W(\Omega = \omega_p, T) = \frac{\pi e^2 a^2}{2\hbar^2 V} K, \quad (6)$$

where  $K$  is the kinetic energy of the carriers,  $a$  is the Cu-O plane lattice parameter, and  $V$  is the LSCO cell volume. In this framework, Eq. (4) derives directly from the Sommerfeld expansion of the Fermi distribution function [17] which, in a first approximation, also gives

$$B(\Omega = \omega_p) \simeq \frac{\pi e^2 a^2}{2\hbar^2 V} \frac{\pi^2 k_B^2}{6} \rho(E_F) \equiv A \frac{\pi^2}{6} \rho(E_F). \quad (7)$$

In two dimensions one may introduce the simplifying assumption of a rectangular density of states, so as  $\rho(E_F) = \rho(E) = (4t_T)^{-1}$ , where  $t_T$  is the hopping rate. Then one finds  $t_T = \pi^2 A / [24B(\omega_p)] = 22 \text{ meV}$  which corresponds to a bandwidth  $8t_T = 176 \text{ meV}$ . By applying the same procedure, even smaller values for  $t_T$  can be extracted from the data [8,15] reported in Fig. 2 for  $\text{Bi}_2\text{Sr}_2\text{CaCu}_2\text{O}_{8+y}$ . On the other hand, applying to the present data Eq. (6), one obtains  $W_0 \simeq 240 \text{ meV}$  for  $x = 0.12$  and  $350 \text{ meV}$  for  $x = 0.26$ . This provides the hopping rate related to the full bandwidth, which we call  $t_0$ . As in any hopping model  $t_0 \lesssim W_0 \lesssim 2t_0$ ,  $t_0$  is in qualitative agreement both with estimates for the Cu-O planes from photoemission data (250–300 meV) [18] and with energy band calculations (430 meV) [19]. However,  $t_0$  is larger, by 1 order of magnitude, than the above  $t_T$  obtained from the

temperature dependence of  $W$ . In the noninteracting description, the two values should be the same. The present inconsistency shows once again that a simple hopping model cannot describe the electrodynamics of the Cu-O planes. One could perform more reliable tight-binding calculations, including the effects of next-nearest neighbor hopping rate  $t'$ , to obtain a different value of  $\rho(E_F)$  and hence of  $t_T$ . However, it is unlikely that such corrections may increase  $t_T$  by an order of magnitude. On the other hand, the possibility that a Van Hove singularity in  $\rho(E)$ , close to the Fermi level, may play a major role in the observed  $T$  dependence of  $W$ , can be excluded. It would imply that  $t_T$  might change very strongly when passing from  $x = 0.12$  to  $0.26$ , in contradiction with the present results at  $\Omega \sim \omega_p$ .

In summary, our results indicate a coexistence of *two different energy scales* in Eq. (5),  $t_0$  and  $t_T$ . The former one is related to the width of the broad conduction band built up either directly by doping or by doping-induced transfer of spectral weight from the high-energy bands [20]. In turn,  $t_T$  seems to control the transfer of spectral weight that is triggered by temperature. From this point of view, one may notice that a similar energy scale is involved in pseudogap formation [1]. However, as the latter phenomenon is restricted to underdoped compounds, that hint should be supported by analyzing the difference in the low-energy thermal response between 0.12 and 0.26, which clearly appears in Fig. 2(b).

The behavior of  $B(\Omega)$  for  $x = 0.12$  in Fig. 2 deserves a few further comments. As the  $T$  dependence of the response is concentrated below  $\sim 4000 \text{ cm}^{-1}$ , the Drude term vanishes at frequencies definitely lower than the pseudoplasma edge at  $\sim 6000 \text{ cm}^{-1}$ . This may explain why this energy is basically insensitive to the number of carriers (in the inset of Fig. 1(c) it is the same for  $x = 0.12$  and  $0.26$ ). A large part of the  $T$ -independent spectral weight  $W_0$  may be ascribed to the midinfrared band peaked at  $\sim 0.5 \text{ eV}$ , directly observed in the semiconducting phase of several cuprates [20] and usually included in the multi-component models of  $\sigma_1^{ab}(\omega)$  as a  $T$ -independent component [21].

The behavior of the spectral weight in the superconducting phase has been studied in the sample with  $x = 0.12$  and, for comparison, in two LSCO single crystals with  $x = 0.10$  and  $0.15$ . Their raw data are reported in Refs. [22] and [3], respectively. We plot in Fig. 3 the difference  $W_n - W_s$  between the spectral weight in the normal phase at  $50 \text{ K}$  and that at a  $T$  well below  $T_c$ . The right-hand panel shows plots of  $(\pi/2)\omega\sigma_2^{ab}(\omega)$ , where  $\sigma_2^{ab}$  is the imaginary part of the in-plane conductivity and is approximately constant, as expected, for  $\omega \leq 250 \text{ cm}^{-1}$ . Its limit for  $\omega \rightarrow 0$  gives the spectral weight which, below  $T_c$ , condenses at  $\omega = 0$  [7,8]. In Fig 3, it coincides for the three samples with the difference  $W_n - W_s$  for  $\Omega \gtrsim 2000 \text{ cm}^{-1}$ . As the gaplike feature in Fig. 2(b) appears around  $200 \text{ cm}^{-1}$ , in LSCO the energy range involved in the FGT sum rule is much larger than

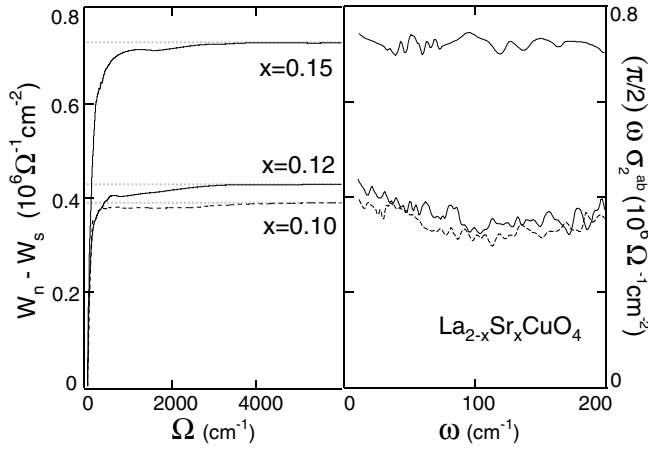


FIG. 3. In the left panel, the difference  $W_n - W_s$  between the spectral weight calculated from  $\sigma_1^{ab}(\omega)$  at 50 K and that at  $T < T_c$  is plotted vs the integration limit  $\Omega$  for  $x = 0.15$  ( $T_c = 41$  K and  $T = 23$  K),  $x = 0.12$  ( $T_c = 29$  K and  $T = 12$  K), and  $x = 0.10$  ( $T_c = 27$  K and  $T = 16$  K). In the right panel  $(\pi/2)\omega\sigma_2^{ab}$  is approximately independent of  $\omega$  for the three samples, as expected, and for  $\omega \rightarrow 0$  provides the spectral weight of the condensate.

expected for a conventional superconductor, as reported for other hole-doped cuprates [8].

From  $W_n - W_s$  one can also extract the London penetration depth  $\lambda_L$ . For the three crystals with  $x = 0.10, 0.12$ , and  $0.15$  of Fig. 2 one obtains 295, 280, and 215 nm, respectively. These values are in good agreement with a previous optical determination in LSCO with  $x = 0.15$  [4] and also with recent muon-spin-rotation measurements [23].

In conclusion, we have used model-independent quantities to compare the infrared response of an underdoped LSCO superconductor and a nonsuperconducting LSCO crystal (indicated in the phase diagram of LSCO as a normal metal) with that of a conventional metal such as gold. In all three samples, the spectral weight  $W(\Omega, T)$  follows the quadratic law  $W = W_0 - B(\Omega)T^2$  for any  $\Omega$  lower than  $\omega_p$ . This allows one to introduce a useful quantity, the thermal response  $B(\Omega)$ . In gold,  $B(\omega_p)$  is reduced to a vanishingly small fraction of its low- $\omega$  value, while in both LSCO samples and in BSCCO  $B(\omega_p)$  is much different from zero. This confirms that the behavior of cuprates is dominated by correlation effects, which extend the energy scale of the restricted sum rule much beyond the plasma edge. We have then applied a single-band hopping model to verify whether  $W_0$  and  $B$  are controlled by the same energy scale, as predicted for normal metals. The result clearly indicates the coexistence of two different energy scales in both LSCO samples,  $t_0$  and  $t_T$ .  $t_0$  is consistent with the bandwidth of photoemission experiments and scales with doping, while  $t_T$  is smaller by 1 order of magnitude. When lowering the

temperature,  $t_T$  controls the transfer of spectral weight in the Drude term towards low frequency. In underdoped samples like the present one with  $x = 0.12$ , this may compete with the opposite transfer corresponding to the opening of a pseudogap [1] since it has the right size ( $\sim 20$  meV or 200 K). This may explain the much smaller variation of  $B$  for low  $\Omega$  at 0.12 than at 0.26, where no pseudogap phenomena are observed. Concerning the superconducting phase, the spectral weight lost below  $T_c$  at  $\omega > 0$  is fully recovered, within errors, by the weight condensed at  $\omega = 0$  in a spectral range of about 0.5 eV. This value is lower than in cuprates with higher  $T_c$ 's, but higher by 1 order of magnitude than in conventional superconductors. The London penetration depth depends on doping and is consistent with muon-spin-rotation values.

We are indebted to L. Benfatto, M. Capone, C. Castellani, M. Grilli, J. Lorenzana, and A. Toschi for many useful discussions. We also wish to thank M. Fujita, K. Yamada, N. Kikugawa, and T. Fujita for providing the LSCO crystals whose optical data have been reanalyzed in the present work.

- [1] For a review, see T. Timusk and B. Statt, Rep. Prog. Phys. **62**, 61 (1999).
- [2] S. Lupi *et al.*, Phys. Rev. Lett. **83**, 4852 (1999), and references therein.
- [3] A. Lucarelli *et al.*, Phys. Rev. Lett. **90**, 037002 (2003), and references therein.
- [4] F. Gao *et al.*, Phys. Rev. B **47**, 1036 (1993).
- [5] S. Tajima *et al.*, cond-mat/0401447 [Phys. Rev. B (to be published)].
- [6] L. Benfatto, S. G. Sharapov, and H. Beck, Eur. Phys. J. B **39**, 649 (2004).
- [7] A. F. Santander-Syro *et al.*, Phys. Rev. Lett. **88**, 097005 (2002).
- [8] H. J. A. Molegraaf *et al.*, Science **295**, 2239 (2002).
- [9] C. C. Homes *et al.*, Phys. Rev. B **69**, 024514 (2004).
- [10] A. V. Boris *et al.*, cond-mat/0405052.
- [11] D. N. Basov *et al.*, Science **283**, 49 (1999).
- [12] M. Ortolani *et al.*, 0407433.
- [13] S. Tajima *et al.*, Phys. Rev. Lett. **91**, 129701 (2003).
- [14] L. Benfatto and C. M. Smith, Phys. Rev. B **68**, 184513 (2003).
- [15] A. F. Santander-Syro *et al.*, Europhys. Lett. **62**, 568 (2003).
- [16] Neither including higher order terms in the Sommerfeld power expansion (4) nor considering fractional power laws appreciably improves the quality of fits to data.
- [17] N. W. Ashcroft and N. D. Mermin, *Solid State Physics* (W. B. Saunders Co., Philadelphia, 1976, p. 47).
- [18] M. R. Norman *et al.*, Phys. Rev. B **52**, 615 (1995).
- [19] E. Pavarini *et al.*, Phys. Rev. Lett. **87**, 047003 (2001).
- [20] S. Uchida *et al.*, Phys. Rev. B **43**, 7942 (1991).
- [21] S. Lupi *et al.*, J. Supercond. **17**, 131 (2004).
- [22] F. Venturini *et al.*, Phys. Rev. B **66**, 060502(R) (2002).
- [23] R. Kadono *et al.*, Phys. Rev. B **69**, 104523 (2004).